Dominant pro-vasopressin mutants that cause diabetes insipidus form disulfide-linked fibrillar aggregates in the endoplasmic reticulum

Julia Birk*, Michael A. Friberg*, Cristina Prescianotto-Baschong, Martin Spiess‡ and Jonas Rutishauser‡,§

Biozentrum, University of Basel, Klingelbergstrasse 70, CH-4056 Basel, Switzerland

*These authors contributed equally to this work
‡These authors contributed equally to this work
§Author for correspondence (j.rutishauser@unibas.ch)

Accepted 21 August 2009
Journal of Cell Science 122, 3994-4002 Published by The Company of Biologists 2009
doi:10.1242/jcs.051136

Summary

Autosomal dominant neurohypophyseal diabetes insipidus results from mutations in the precursor protein of the antidiuretic hormone arginine vasopressin. Mutant prohormone is retained in the endoplasmic reticulum of vasopressinergic neurons and causes their progressive degeneration by an unknown mechanism. Here, we show that several dominant pro-vasopressin mutants form disulfide-linked homo-oligomers and develop large aggregations visible by immunofluorescence and immunogold electron microscopy, both in a fibroblast and a neuronal cell line. Double-labeling showed the pro-vasopressin aggregates to colocalize with the chaperone calreticulin, indicating that they originated from the endoplasmic reticulum. The aggregates revealed a remarkable fibrillar substructure. Bacterially expressed and purified mutant pro-vasopressin spontaneously formed fibrils under oxidizing conditions. Mutagenesis experiments showed that the presence of cysteines, but no specific single cysteine, is essential for disulfide oligomerization and aggregation in vivo. Our findings assign autosomal dominant diabetes insipidus to the group of neurodegenerative diseases associated with the formation of fibrillar protein aggregates.

Key words: Aggregates, Diabetes insipidus, Fibrils, Neurophysin, Vasopressin

Introduction

Familial neurohypophyseal diabetes insipidus, a disorder of water homeostasis, results from lack of the circulating antidiuretic hormone vasopressin, normally produced in vasopressinergic neurons in the hypothalamic magno- and parvocellular nuclei. As a consequence, vasopressin-mediated reabsorption of water from the renal collecting ducts is deficient, causing patients to lose large amounts of unconcentrated urine and to suffer from increased thirst. The disease is caused by mutations in the gene encoding the vasopressin pre-prohormone. The vasopressin precursor consists of a signal peptide of 19 amino acids, the nine-amino acid hormone, a three-amino acid linker, the 93-amino acid carrier protein neurophysin II (NPII), a single linker amino acid and a C-terminal glycopeptide of 39 amino acids (Fig. 1). The precursor is stabilized by the formation of eight disulfide bridges, one in the hormone and seven in the NPII moiety.

Over 50 pathogenic mutations of the human vasopressin gene have been reported that alter the signal peptide, the hormone, or the NPII moieties (Christensen and Rittig, 2006). So far, no mutations have been found in the glycopeptide. Almost all mutations are dominant. Only the P7L mutant (Pro7 of vasopressin mutated to Leu; Willcutts et al., 1999) causes a recessive form of the disease. Autosomal dominant neurohypophyseal diabetes insipidus (ADNDI) shows a high penetrance, with symptoms beginning weeks to months after birth. Postmortem histological studies of affected individuals have shown degeneration of the vasopressinergic magnocellular neurons (Bergeron et al., 1991; Braverman et al., 1965; Green et al., 1967; Nagai et al., 1984). A knock-in mouse model expressing the human pathogenic mutant C67X (Cys67 of NPII mutated to a stop codon) confirmed the neurotoxic effect of the mutant protein on vasopressinergic cells (Russell et al., 2003), but the mechanism causing cell death remains unknown.

Expression studies have shown that dominant pro-vasopressin mutants are not secreted, but are retained in the endoplasmic reticulum (ER) (Beuret et al., 1999; Christensen et al., 2004; Friberg et al., 2004; Ito and Jameson, 1997; Nijenhuis et al., 1999; Olias et al., 1996; Siggaard et al., 1999). Most of the retained mutant protein is degraded by cytosolic proteasomes after retrotranslocation (Friberg et al., 2004). Here, we show that newly synthesized mutant precursors form disulfide-linked homo-oligomers and large ER-derived accumulations with a fibrillar ultrastructural appearance. Fibril formation was reproduced by the purified precursor in vitro. The results suggest that disulfide-linked oligomers in part escape degradation and gradually aggregate. Autosomal dominant diabetes insipidus thus belongs to the neurodegenerative diseases associated with fibrillar protein aggregation.

Results

Secretion-deficient dominant mutants form disulfide-linked homo-oligomers

To assay for secretion, wild-type pro-vasopressin, the recessive mutant P7L, and the dominant mutants ΔE47, Y2H, C28Y and ΔG227 were expressed in COS-1 cells, pulse-labeled with [^{35}S]methionine/cysteine, chased for 2 hours, isolated from the cells and from the media by immunoprecipitation, and analyzed by SDS-gel electrophoresis and autoradiography (Fig. 2A). As expected, a considerable fraction of the wild type and of P7L was recovered from the media, reflecting their ability to fold and pass ER quality control. By contrast, the dominant mutants ΔE47, Y2H and C28Y

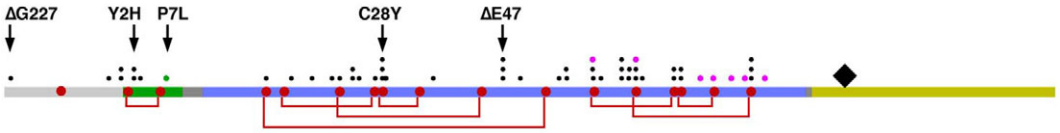

Fig. 1. Wild-type and mutant vasopressin precursors. The domain organization of the vasopressin precursor (signal sequence in gray, vasopressin in green, NPII in blue, glycopeptide in yellow) is shown with cysteine residues as red dots, disulfide bridges as red lines, and the glycosylation site as a black diamond. The positions of known ADNDI mutations are indicated as dots above the sequence (black for missense, pink for stop codon mutations). The only recessive mutation is indicated by a green dot. The mutations analyzed in this study are indicated by arrows.

were completely retained in the cells. Only the dominant mutant ΔG227, in which the signal sequence is inefficiently cleaved, was also partially secreted (Fig. 2A, lanes 13 and 14). The reduced molecular weight of the secreted protein indicates that the uncleaved pre-pro-vasopressin was retained and only cleaved pro-vasopressin, which is identical to wild type, was allowed to exit.

We have previously observed the formation of disulfide-linked products of retained ΔG227 in COS cells (Beuret et al., 1999). Here, we investigated the formation of disulfide complexes for the wild-type and all five pro-vasopressin mutants in COS-1 and Neuro2a mouse neuroblastoma cells. Transiently transfected cells were radiolabeled with [^{35}S]methionine/cysteine for 1 hour and then incubated with iodoacetamide to alkylate free SH-groups and prevent post-lysis oxidation. Vasopressin precursors were immunoprecipitated and separated by gel electrophoresis either under non-reducing conditions or after reduction of disulfide bonds with β-mercaptoethanol. Under reducing conditions, the precursors expressed in Neuro2a cells were found as a ~21 kDa species representing glycosylated pro-vasopressin (Fig. 2B). By contrast, non-reducing conditions (Fig. 2C) revealed a ladder of bands corresponding in size to prohormone oligomers. Whereas wild-type pro-vasopressin and the recessive mutant P7L produced less than 20% of high molecular weight forms, most of the dominant mutant proteins (50-90%) were found in covalent oligomers (Fig. 2D). Qualitatively the same result was obtained with expression in COS-1 cells (not shown), indicating that disulfide-linked oligomerization of mutant pro-vasopressin is not a phenomenon specific to neuronal cells.

The strikingly regular spacing of the disulfide-linked products suggested homo-oligomerization of the precursor protein. To test this hypothesis, a lane containing the non-reduced ΔE47 products was cut out, placed horizontally onto a second gel, and overlaid with reducing sample buffer before electrophoresis. All disulfide-linked oligomers collapsed to bands of the same mobility as the monomeric protein (Fig. 2E). The same result was observed for the ΔG227 mutant (not shown). The disulfide-linked products generated predominantly by the dominant mutants thus represent homo-oligomers of glycosylated vasopressin precursor.

Dominant pro-vasopressin mutants progressively accumulate as ER-associated aggregates

To characterize the intracellular localization of the vasopressin precursors, transfected COS-1 cells were analyzed by immunofluorescence staining 48 hours after transfection (Fig. 3). COS cells are particularly suitable for visualizing intracellular organelles and aggregations due to their flat cell body and large cytoplasm. As previously shown (Beuret et al., 2004), expression of regulated secretory proteins such as granins and prohormones, including pro-vasopressin, is sufficient to generate granule-like structures in a variety of nonendocrine cell lines due to aggregation in the trans-Golgi. Accordingly, wild-type precursor was concentrated in granular accumulations in the cell periphery of about half the expressing cells (Fig. 3A). The recessive mutant P7L

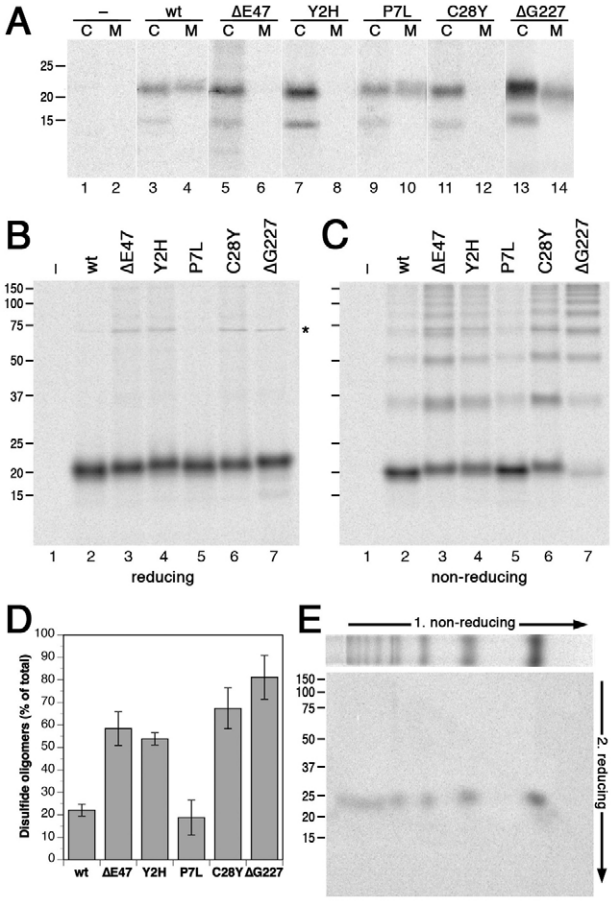

Fig. 2. Disulfide-linked pro-vasopressin homo-oligomers. (A) Wild-type (wt) vasopressin precursor and the mutants ΔE47, Y2H, P7L, C28Y and ΔG227 were expressed in COS-1 cells, pulse-labeled with [^{35}S]methionine/cysteine for 1 hour, and chased for 2 hours. Pro-vasopressin was immunoprecipitated from cell lysates (C) and media (M), and analyzed by SDS-gel electrophoresis and autoradiography. The positions of marker proteins are indicated with their molecular masses in kDa. (B-E) Untransfected Neuro2a cells (–) and cells expressing wild-type (wt) or mutant vasopressin precursor were pulse-labeled and immunoprecipitated. Precursors were analyzed after reduction of disulfide bonds (B) or under non-reducing conditions (C) by SDS-gel electrophoresis and autoradiography. The asterisk indicates the position where the spacer gel ends and the separating gel begins. (D) The fraction of disulfide-linked oligomers as a percentage of the total protein (mean ± s.d. of three independent experiments). (E) ΔE47 products were separated in a first dimension by non-reducing gel electrophoresis and subjected to a second gel electrophoresis after reduction of disulfide bonds.

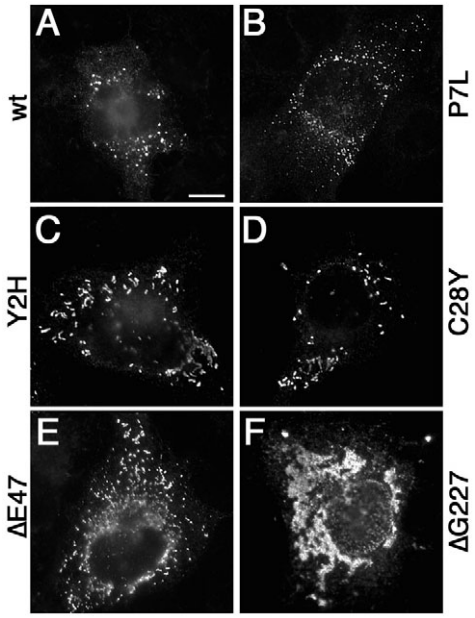

Fig. 3. Intracellular accumulation of wild-type and mutant pro-vasopressin in COS-1 cells. COS-1 cells expressing wild-type pro-vasopressin or the indicated mutants were subjected to immunofluorescence staining against NPII 48 hours post-transfection. (A,B) As expected, approximately half the cells expressing wild-type pro-vasopressin or P7L produced mostly round granule-like structures. (C-F) Dominant mutants showed accumulations that were mostly elongated or laminar. The different shapes did not correlate with specific mutations. Scale bar: 20 μm.

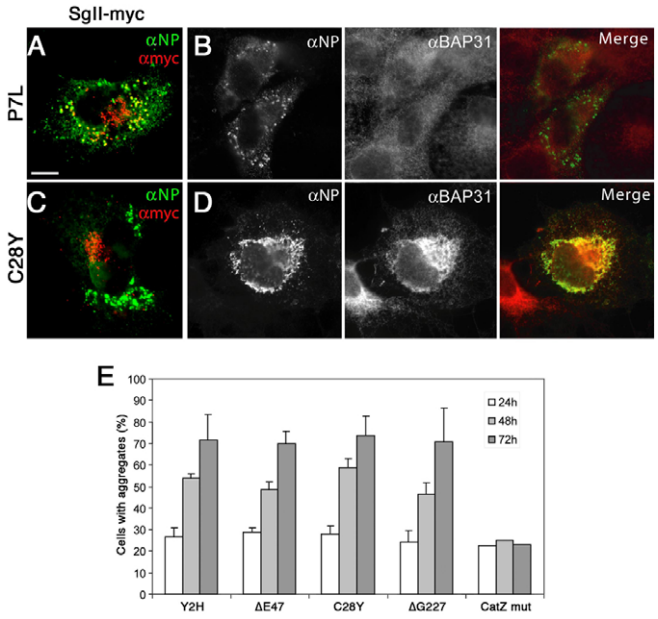

Fig. 4. Gradual development of aggregations of dominant pro-vasopressin mutants in the ER. COS-1 cells expressing the recessive pro-vasopressin mutant P7L (A,B) or the dominant mutant C28Y (C,D) were stained 48 hours post-transfection for NPII in green, and either for cotransfected secretogranin II-myc (SgIImyc; A,C) as a marker for granule-like structures, or against endogenous BAP31 (B,D) in red. Scale bar: 20 μm. (E) COS-1 cells transfected with each of the four dominant pro-vasopressin mutants were analyzed by immunofluorescence staining after 24, 48 or 72 hours and the cells with visible aggregates of any kind were quantified. As a control, the experiment was performed in parallel for a mutant cathepsin Z (CatZ mut), another ER-retained secretory protein. Bars indicate mean ± s.d. of three independent experiments.

showed the same immunofluorescence pattern as the wild type (Fig. 3B), which is in agreement with the observation that P7L was not retained in the ER, but was secreted into the culture medium as was the wild-type prohormone (Fig. 2A).

In many cells, the dominant mutants showed strong reticular staining typical for proteins retained in the ER. However, in up to 60% of the transfected cells, they also produced condensed accumulations dispersed throughout the cell (Fig. 3C-F), with morphologies distinct from that of the granule-like structures formed by the wild-type protein or the recessive P7L mutant. These accumulations had a coarse, short tubular (Fig. 3C-E) or irregular, laminar appearance (Fig. 3F). The different morphologies of the aggregates were not specific to particular mutants, but were found for all of them. The accumulations were distinct from mitochondria as there was no co-staining with the mitochondrial marker cytochrome *c* (not shown).

To unambiguously distinguish between granule-like structures and accumulations formed in the ER, co-staining experiments were performed. When wild-type pro-vasopressin and other regulated secretory proteins (e.g. secretogranin II) were co-expressed in COS-1 cells, they colocalized in granule-like structures (Beuret et al., 2004). This was also the case for the P7L mutant (Fig. 4A). By contrast, the secretogranin structures and the accumulations of the dominant mutants were clearly distinct (shown in Fig. 4C for C28Y). When COS-1 cells expressing pro-vasopressin were co-stained with antibodies against NPII and against BAP31 (B-cell receptor-associated protein 31; an endogenous ER membrane protein), the granule-like structures of P7L [like those of the wild type (Beuret et al., 2004)] were not positive for BAP31 (Fig. 4B). By contrast, there was extensive co-staining of the C28Y accumulations with BAP31 (Fig. 4D), indicating that the aggregations produced by the dominant mutant are located within the ER. The same was observed with all dominant mutants.

COS-1 cells transfected with the four dominant mutants were analyzed by immunofluorescence at different times after transfection (Fig. 4E). All mutants produced similar results. At 24 hours after transfection, anti-NPII immunostaining showed the reticular ER pattern, identical to that produced by anti-BAP31 antibody staining, in a majority of the cells, whereas less than 30% of transfected cells showed distinct aggregates. After 48 and 72 hours, the percentage of aggregate-forming cells increased to ~55% and ~75%, respectively, and the aggregations generally increased in size. As a control, we also analyzed the immunofluorescence staining of COS-1 cells expressing an ER-retained mutant of cathepsin Z, a secretory protein with five disulfide bonds. In these experiments, the frequency of apparent aggregations did not increase with time above the control levels of ~20%. Large aggregates and disulfide oligomers were also produced by dominant vasopressin mutants expressed in CV-1 cells (the parental cell line of COS-1 cells) lacking the large T-antigen needed for high-level expression (not shown). Thus, the formation of aggregates was not an artifact of excessive expression levels due to plasmid amplification.

Mutant pro-vasopressin aggregates show filamentous ultrastructure

COS-1 cells expressing dominant mutants were analyzed by immunogold electron microscopy 48 hours after transfection (Fig. 5).

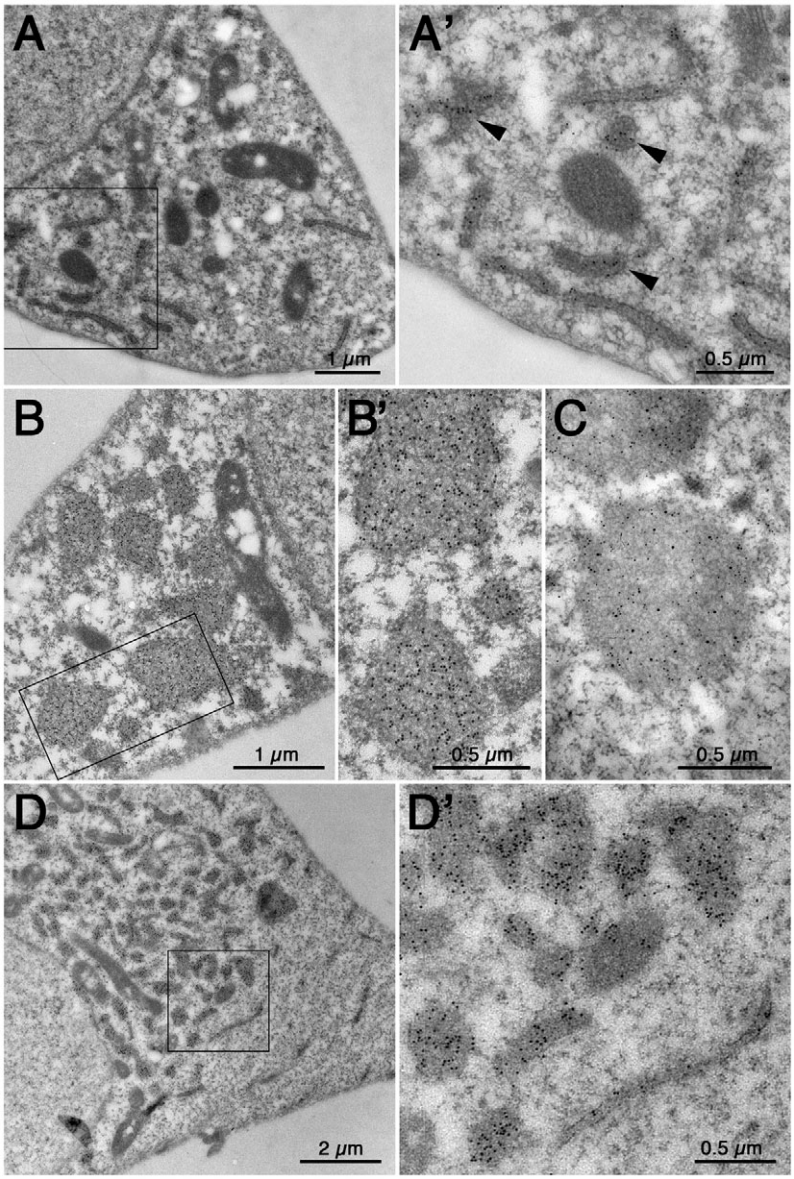

Fig. 5. Mutant pro-vasopressin aggregations in COS-1 cells visualized by electron microscopy. COS-1 cells transfected with ΔE47 (A-C) or ΔG227 (D) were analyzed by immunogold electron microscopy using 15-nm gold to decorate pro-vasopressin. (C) The section was also double-labeled with 10-nm gold for the ER chaperone, calreticulin. Boxed areas in A, B and D are shown as enlargements in A′, B′ and D′. Arrowheads in A′ point out dilated ER elements.

As expected, gold staining was found in many cells in ER tubules cut longitudinally or across, some of which had a dilated appearance (Fig. 5A,A′). Other cells contained multiple large structures of ~1 μm in diameter decorated with 15-nm gold for pro-vasopressin (Fig. 5B,B′,C), corresponding to the bright accumulations seen by immunofluorescence (Fig. 3C,D,E). In some cells, large regions were densely filled with labeled structures (Fig. 5D,D′) that might appear almost continuous in immunofluorescence (as in Fig. 3F), adjacent to regions with normal-sized ER tubules of ~60-90 nm diameter. With double-labeling, the pro-vasopressin aggregations stained for NPII with 15-nm gold were also found to be decorated with 10-nm gold for the ER chaperone calreticulin (Fig. 5C), confirming that these are ER-derived structures. In some micrographs, the core of the aggregates appeared to be structured, and gold particles were aligned in continuous rows (Fig. 5B′), suggesting a filamentous arrangement of the antigen.

To also test their behavior in a neuronal cell type representing the physiological situation more closely, dominant pro-vasopressin mutants were expressed in Neuro2a cells and analyzed by immunofluorescence and electron microscopy. By confocal microscopy, dispersed accumulations of pro-vasopressin could again be observed that were strongly co-stained for the ER chaperone Hsp47 (heat shock protein 47; Fig. 6). At the ultrastructural level, immunogold staining showed pro-vasopressin in compact accumulations of similar size to those in COS-1 cells (Fig. 7A and enlarged areas in Fig. 7B,C). The aggregations are structured and appear to be composed of tangled filaments of approximately 10-15 nm diameter (Fig. 7B-F). Using double-labeling, both mutant pro-vasopressin and calreticulin were again found to decorate these structures (Fig. 7D,F), demonstrating that they are derived from the ER. Clearly, aggregations containing mutant pro-vasopressin are formed not only in fibroblasts, but also in neuronally derived cells, which better mimic the pathological situation in vivo.

Purified pro-vasopressin spontaneously forms fibrils after removal of denaturant

To test the ability of pro-vasopressin to form fibrils in isolation, the ΔE47 mutant was expressed with a C-terminal His6 tag replacing

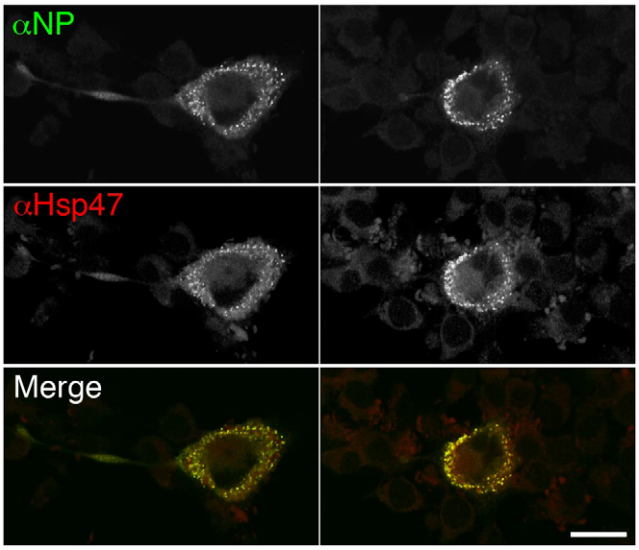

Fig. 6. Accumulation of mutant pro-vasopressin in Neuro2a cells. Differentiated Neuro2a cells expressing C28Y pro-vasopressin were stained 48 hours post-transfection for NPII in green, and for the ER chaperone Hsp47 in red, and analyzed by confocal microscopy. Scale bar: 20 μm.

the signal sequence in *Escherichia coli*, recovered in inclusion bodies, solubilized with 8 M urea, and purified under reducing conditions by metal-chelate affinity chromatography. After removal of urea and reducing agent by dialysis, and pelleting of amorphous precipitates by centrifugation, fibrillar structures of defined diameter were detected in the supernatant by electron microscopy (Fig. 8). No fibrils were observed when reducing conditions were maintained throughout. These results show that pro-vasopressin can form fibrils in vitro in the absence of any other cellular proteins and that oxidation is necessary to stabilize them.

Cysteine residues are required for aggregate formation

To investigate whether the formation of disulfide-linked oligomers and of large aggregations is dependent on specific cysteine residues, we generated artificial mutants in which the cysteines in any of four segments of the precursor protein were replaced by serines, or in which all 16 cysteines were mutated (Fig. 9A). Mutation of cysteines almost certainly prevents native folding of the precursor (10 of the 16 have been found mutated in diabetes insipidus alleles). These mutants were tested for the formation of disulfide-linked oligomers in Neuro2a cells (Fig. 9B,C) and of aggregates in COS-1 cells (Fig. 9D,E). Mutation of any one group of cysteines still allowed efficient formation of disulfide oligomers and the appearance of large aggregations. None of the cysteines is thus essential for disulfide oligomerization or aggregation. As expected, the mutant without any

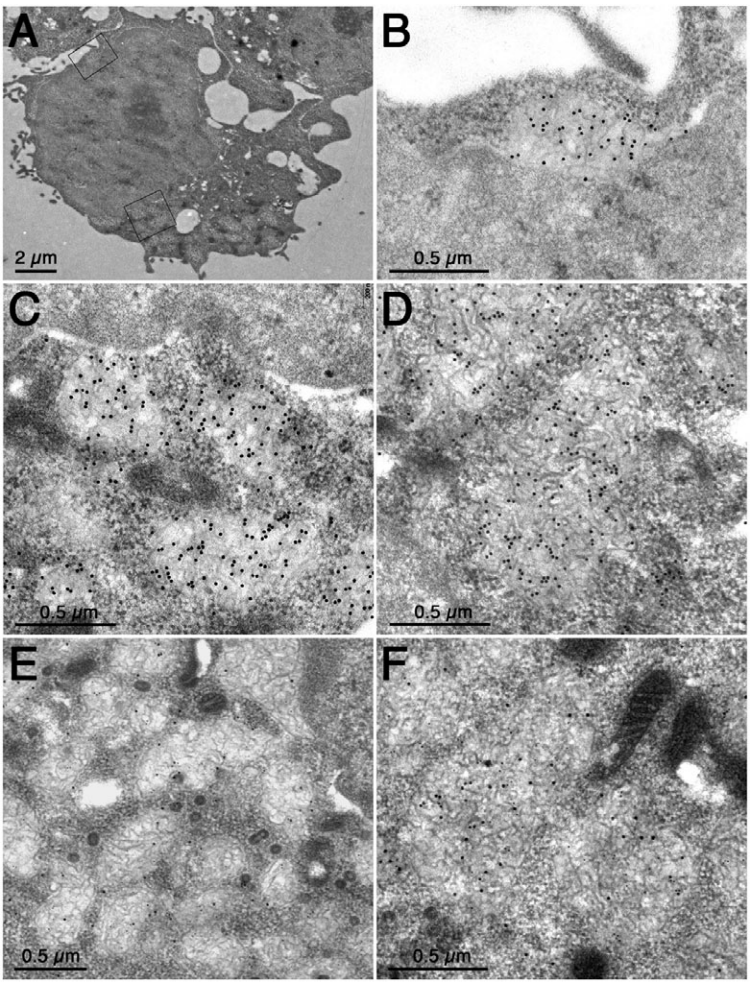

Fig. 7. Fibrillar ultrastructure of mutant pro-vasopressin aggregations in Neuro2a cells. Immunogold electron microscopy of Neuro2a cells expressing ΔE47. (A-D) Pro-vasopressin was stained with 15-nm gold. (E,F) In addition to the pro-vasopressin staining, the ER marker calreticulin was stained with 10-nm gold. Boxed areas in A are shown as enlargements in B and C.

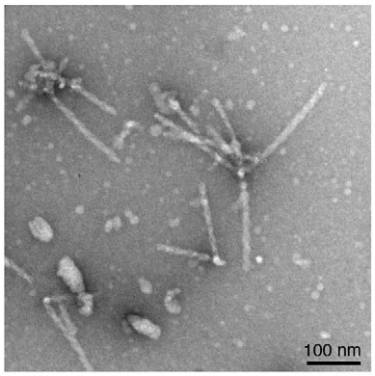

Fig. 8. In vitro formation of fibrils from purified pro-vasopressin ΔE47. Bacterially expressed pro-vasopressin ΔE47 with a C-terminal His6-tag was purified by metal-chelate affinity chromatography in 8 M urea and 1 mM DTT. After removal of urea and DTT (as described in Materials and Methods), fibrils of defined diameter were visualized by electron microscopy.

cysteines did not produce covalent homo-oligomers (Fig. 9B, abcd). Also, this cysteine-less mutant did not induce the formation of aggregates detectable by immunofluorescence (Fig. 9D,E). When these mutants were tested for ER retention, two constructs, aBCD and abcd, were surprisingly found to be partially secreted into the medium (Fig. 9G, lanes 10 and 14).

To exclude the possibility that the absence of aggregates with construct abcd is due to reduced ER concentrations, the ER retention signal KDEL was fused to the C-terminus. This effectively prevented secretion of both $aBCD^{KDEL}$ and $abcd^{KDEL}$ (lanes 12 and 16). The cysteine-less construct, even when retained in the ER as $abcd^{KDEL}$, did not increase aggregate formation above backgound levels (Fig. 9D,E). Even at the ultrastructural level, no aggregations could be observed for abcd but there was dispersed staining in the ER (mostly tubular elements in the cytosol and the nuclear envelope; Fig. 9F).

To test the ability of the cysteine-free construct to form fibrils in vitro, abcd without the signal sequence was expressed in bacteria. Unlike ΔE47 pro-vasopressin, which accumulated in inclusion bodies, abcd remained soluble in the bacterial cytoplasm. After purification in 8 M urea, dialysis to remove the denaturant and dithiothreitol (DTT), and analysis by electron microscopy, hardly any structures resembling the fibrillar aggregates found for ΔE47 in a parallel experiment could be detected (not shown). Together with the in vivo results this suggests that, whereas no individual cysteine in the precursor is necessary for oligomerization or aggregation, the formation of fibrils and aggregates is dependent on the presence of cysteine residues, irrespective of their positions within the precursor protein.

Discussion

Dominant pro-vasopressin mutants cause ER retention due to misfolding

Many different mutations in the vasopressin precursor have been shown to cause diabetes insipidus. Only two of these are recessive. The human P7L mutation in the vasopressin nonapeptide (Willcutts et al., 1999) greatly reduces hormone binding to its renal receptor, but does not affect precursor folding and secretion. In addition, the Brattleboro mutation in rat, a frameshift mutation in the gene segment encoding NPII, shows a recessive phenotype (Schmale and Richter, 1984). Here, the complete absence of a stop codon in the new reading frame results in highly inefficient translation of the mutant protein, resulting essentially in a null allele. All other known mutations in the vasopressin precursor are dominant, eventually causing death of the vasopressin-producing neurons.

The mutations are diverse and not localized to a specific region in the precursor protein, except that no pathogenic mutations have been identified within the C-terminal glycopeptide. Cytotoxicity appears therefore not to be caused by a specific effect of each individual mutation within the prohormone, but to result from consequences common to all the mutations. This notion is supported by two mutations in the signal sequence, ΔG227 (resulting in a signal truncation; Beuret et al., 1999) and A(–1)T (mutation of the signal cleavage site; Ito et al., 1993). In both cases, removal of the signal peptide is impaired, but the pro-vasopressin sequence itself remains unchanged. A common effect of all dominant mutants tested is their retention in the ER, most probably due to misfolding. For frameshift and point mutations affecting cysteine residues normally involved in disulfide bonds, misfolding is an obvious consequence. Failure to cleave the signal sequence has a more subtle effect, as it prevents the N-terminus of the vasopressin sequence from folding into NPII, a requirement for the stabilization of the disulfide bond within the hormone segment (Beuret et al., 1999; Chen et al., 1991). How can misfolding and ER retention cause cytotoxicity?

Mutant pro-vasopressins form disulfide-linked homo-oligomers, fibrils and large aggregations

At least half of the newly synthesized precursor proteins of all four dominant mutants were found to be part of disulfide-linked homo-oligomers. This indicates a specific interaction between unfolded pro-vasopressin polypeptides, bringing together cysteines to form intermolecular crosslinks. Using in vitro mutagenesis, we tested which cysteines might be essential for this process. Whereas the presence of some cysteines was required for the formation of disulfide-linked oligomers as well as aggregations visible by immunofluorescence, no single cysteine was specifically necessary.

Disulfide-linked homo-oligomers were also observed for wild-type pro-vasopressin and the recessive mutant P7L, but to a much lower extent. Not-yet folded protein appears to be transiently crosslinked into disulfide-linked homo-oligomers, but to be subsequently rescued when the free molecules successfully fold into the native structure. Indeed, even the mutant proteins are not irreversibly trapped in disulfide aggregates because we have previously found them to be quite efficiently degraded by the cytosolic proteasome (Friberg et al., 2004). Only a small fraction thus escapes ER-associated degradation to accumulate in large aggregates visible by fluorescence and electron microscopy. Consistent with this, it takes 2-3 days for a majority of expressing cultured cells to develop visible aggregates.

Electron microscopic analysis showed that the pro-vasopressin accumulations have a fibrillar ultrastructure. The ability of pro-vasopressin to form ordered, linear polymers by self-assembly was confirmed in vitro with bacterially expressed and purified protein. The vasopressin precursor thus resembles a whole family of proteins that generate amyloid fibers and are associated with neurodegenerative disorders.

A model for the formation of fibrillar aggregates in the ER

Taken together, our results suggest a model for aggregate formation in ADNDI as illustrated in Fig. 10. After translocation into the ER lumen, vasopressin precursor might acquire a conformation that

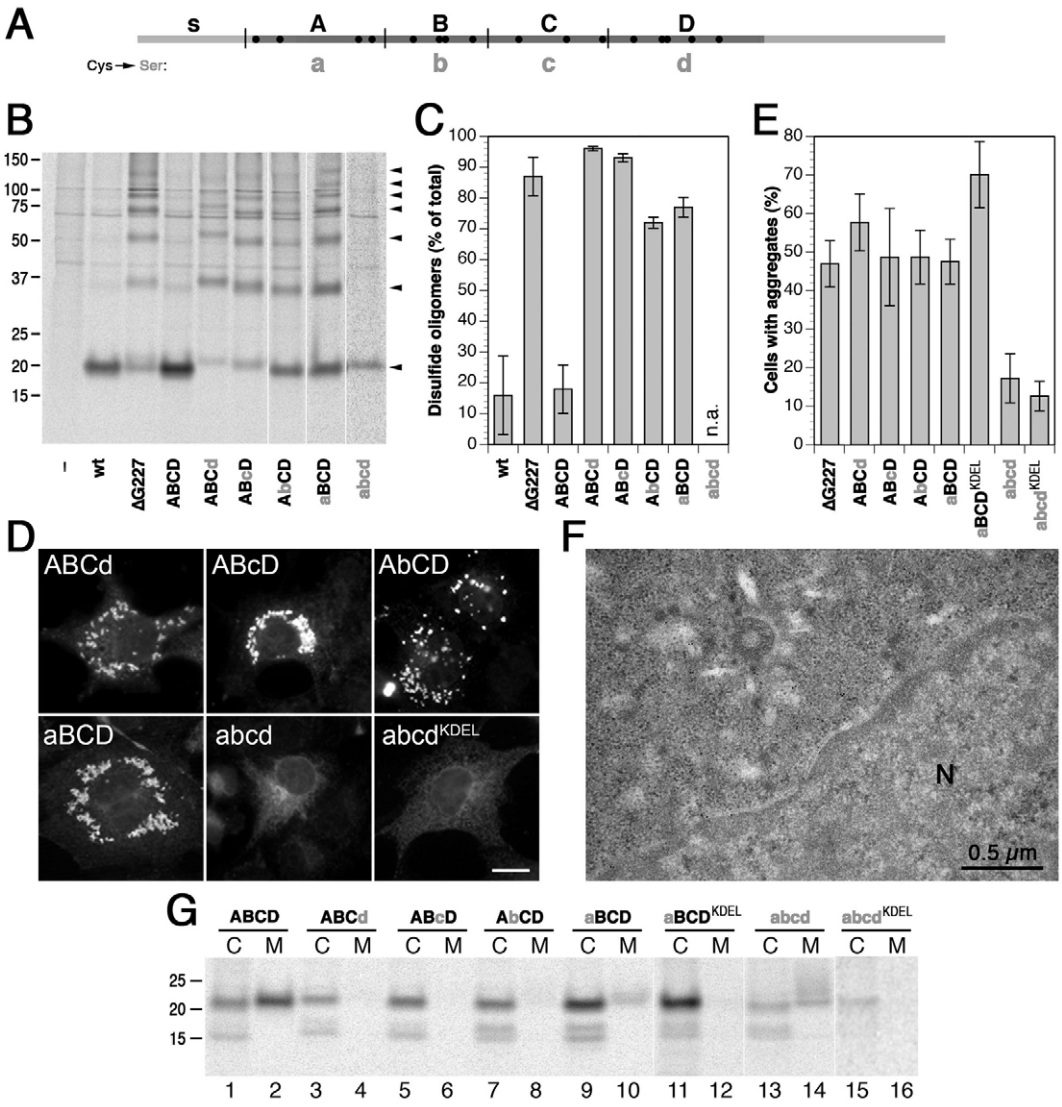

Fig. 9. Contribution of cysteine residues to the formation of aggregates. (A) The 16 cysteines in pro-vasopressin (indicated as black dots) were mutated in groups corresponding to four segments (A, B, C, D) to serines (a, b, c, d). s indicates the signal sequence (in these constructs, the pre-pro-enkephalin signal replaced the natural signal peptide). (B) To analyze the formation of disulfide-linked oligomers, Neuro2a cells were transfected with the indicated constructs and labeled for 1 hour with [^{35}S]methionine/cysteine. After alkylation of free SH groups, pro-vasopressin was immunoprecipitated and analyzed by SDS-gel electrophoresis under non-reducing conditions. The experiment with untransfected cells (–) reveals the non-specific bands. The positions of molecular mass standards (in kDa) are indicated. The absence of cysteines in construct abcd (with a single methionine in NPII) accounts for its low labeling signal. (C) The signal of homo-oligomers (arrowheads in panel B; but not applicable for abcd) were quantified and shown as a percentage of the total (mean ± s.d. of three independent experiments). No specific cysteine cluster was necessary for the formation of oligomers. (D) COS-1 cells expressing the indicated constructs were analyzed by immunofluorescence microscopy after staining for pro-vasopressin 2 days after transfection. Typical examples are shown. Scale bar: 20 μm. (E) The frequency of aggregate formation was quantified from immunofluorescence micrographs as shown in panel D (mean ± s.d. of three independent experiments). Wild-type pro-vasopressin from the original cDNA (wt) or from the cDNA containing silent mutations introducing additional restriction sites (ABCD) produced post-Golgi granule-like structures and were not included in this analysis. Background as determined for mutant CatZ in Fig. 4E is ~15-20%. (F) Electron micrograph of a Neuro2a cell expressing the cysteine-free construct abcd stained for pro-vasopressin with 15-nm gold. Distributed staining on the nuclear envelope and cytoplasmic ER is observed, but no aggregations. N, nucleus. (G) Secretion of the cysteine mutants expressed in COS-1 cells was analyzed in a pulse-chase experiment as in Fig. 2A. Constructs aBCD^{KDEL} and abcd^{KDEL} correspond to aBCD and abcd with a C-terminal ER retention sequence.

leads to homo-oligomers, which are stabilized by intermolecular disulfide-links between exposed cysteine residues. This process is reversible and thus allows wild-type proteins to fold into their native structure and exit the ER, and allows folding-deficient mutants to be retrotranslocated into the cytosol for proteasomal degradation. A significant fraction of mutant precursors accumulate as growing oligomers and polymers, forming fibrils and eventually large visible aggregates associated with ER chaperones.

Role of aggregates for cytotoxicity

The formation of fibrillar aggregations and inclusion bodies are frequent pathological features of neurodegenerative disorders (Ross and Poirier, 2005). In contrast to the extensively studied aggregations associated with Alzheimer's, Parkinson's and Huntington's disease that are extracellular, cytoplasmic or intranuclear, the aggregations formed by dominant pro-vasopressin mutants are produced within the lumen of the ER.

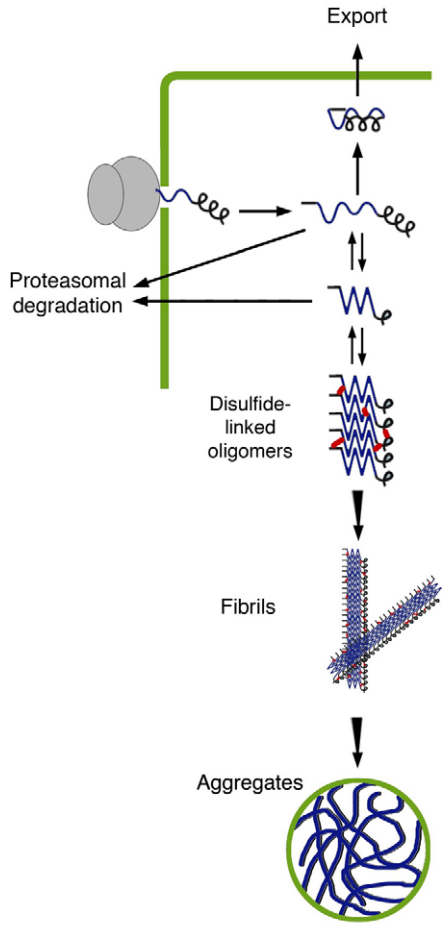

Fig. 10. Model for the development of fibrillar aggregates in the ER. Pre-pro-vasopressin is synthesized by the ribosome (gray structure) into the ER to undergo folding and quality control. A part of the precursor sequence (in blue) can assume alternative conformations, potentially leading to aggregation. Natively folded precursor leaves the ER and exits the cell via the secretory pathway and secretory granules. Misfolded precursor might either be retrotranslocated for subsequent proteasomal degradation, or form specific oligomers and polymers that are stabilized by disulfide links (in red). Polymers grow into fibrils and generate inclusions within the ER that are visible by light microscopy. ER membrane is shown in green.

The role of aggregation in degenerative disease processes is controversial because there is often no direct correlation between the amount of inclusions and cell degeneration (Chun et al., 2002; Ross and Poirier, 2005). The formation of large aggregates and inclusion bodies might represent a cellular protective response, and early protofibrils might be the neuropathogenic species triggering disease (Lansbury and Lashuel, 2006; Ross and Poirier, 2005). In a diabetes insipidus knock-in mouse expressing the cytotoxic pro-vasopressin mutant C67X, induction of the ER chaperone BiP was detected, but no obvious aggregations were apparent (Russell et al., 2003). No upregulation of the ER stress-induced pro-apoptotic transcription factor C/EBP homologous protein (CHOP) or other evidence for apoptosis was observed. However, aggregate-producing cells might have been rapidly eliminated. By contrast, vasopressinergic neurons expressing the same C67X mutant in transgenic rats were resistant to a cytotoxic effect, but produced distended ER structures containing the mutant protein and markers of autophagy (Davies and Murphy, 2002; Si-Hoe et al., 2000). This lysosomal degradation mechanism is thought to protect against the toxic effects of altered or aggregated intracellular proteins (Martinez-Vicente and Cuervo, 2007). Inhibition of autophagy was found to compromise the viability of C67X-expressing rat neurons and Neuro2a cells (Castino et al., 2005). Interestingly, we could not detect significant colocalization of the dominant mutant C28Y with Lamp1 or LC3 (markers for lysosomes and autophagosomes, respectively) neither in COS-1 nor Neuro2a cells (J.B., unpublished). The extent to which the disulfide-linked homo-oligomers of pro-vasopressin mutants detected biochemically and the large aggregations observed by light and electron microscopy contribute to cytotoxicity remains to be analyzed in detail.

Materials and Methods

Plasmids and constructs

The cDNAs of the human wild-type vasopressin precursor and the mutants ΔG227, ΔE47 and C67X, as well as of myc-tagged secretogranin II, have been described before (Beuret et al., 1999; Friberg et al., 2004). The cDNAs encoding the vasopressin mutants Y2H and P7L were a gift from Jane Christensen (Århus University Hospital, Aarhus, Denmark). The C28Y mutant was generated by polymerase chain reaction. The expression plasmid of human pre-pro-cathepsin Z mutant (N184Q, N224Q) (Appenzeller-Herzog et al., 2005) was a gift from Hans-Peter Hauri and Beat Nyfeler (Biozentrum, University of Basel, Basel, Switzerland). All human cDNAs were subcloned into the pRc/RSV expression plasmid (Invitrogen).

The 16 cysteine residues in pro-vasopressin were mutated to serines by PCR mutagenesis. For this purpose, the signal sequence was replaced by that of pre-pro-enkephalin as described (Cescato et al., 2000; Friberg et al., 2004), providing a *Bsr*GI restriction site near the start of pro-vasopressin. Silent mutations were introduced to insert a *Kpn*I site at codons 49/50 of the pro-vasopressin coding sequence and a *Bam*HI site at codons 64/65. Together with a natural *Sma*I site at codons 27/28 and external *Sal*I site, these restriction sites served to clone and recombine PCR-amplified mutant segments. All constructs were verified by DNA sequencing.

Cell culture and transient transfection

COS-1 cells were grown in Dulbecco's modified Eagle's medium (DMEM; Sigma) supplemented with 10% fetal calf serum (FCS), 100 units/ml penicillin, 100 μg/ml streptomycin and 2 mM L-glutamine at 37°C in 7.5% CO_2. COS-1 cells were transiently transfected in six-well plates using Lipofectine (Invitrogen) or FuGENE HD (Roche) and analyzed 2-3 days after transfection or as indicated. Neuro2a cells were grown in DMEM containing 4500 mg/l glucose, supplemented as above. They were transfected using Metafectene (Biontex Laboratories). To induce differentiation, cells were cultured from 1 day before transfection in 1 mM valproic acid in DMEM with 3% FCS, 100 units/ml penicillin, 100 μg/ml streptomycin and 2 mM L-glutamine.

Metabolic labeling and immunoprecipitation

For labeling experiments, transfected cells were starved for 30 minutes in DMEM without methionine and cysteine (Sigma), supplemented with 2 mM L-glutamine. Cells were labeled with 100 μCi/ml [^{35}S]protein-labeling mix (PerkinElmer) and chased with excess methionine and cysteine. Cells were washed in phosphate-buffered saline (PBS), lysed in 500 μl of lysis buffer (PBS, 1% TritonX-100, 0.5% deoxycholate, 2 mM phenylmethylsulfonylfluoride), and scraped. Cell lysates or media were incubated with rabbit polyclonal anti-NPII (Friberg et al., 2004) in lysis buffer containing 1 mM phenylmethylsulfonylfluoride, 0.5% SDS and 1 mg/ml BSA. Bound proteins were immunoprecipitated with protein-A–Sepharose (Zymed) and analyzed by electrophoresis on 10% polyacrylamide Tris/tricine SDS-gels and autoradiography.

Analysis of disulfide-linked oligomers

Transfected and labeled cells were washed with cold PBS containing 100 mM iodoacetamide; incubated at 4°C for 1 hour in the dark with 200 μl 200 mM Tris pH 8.0, 100 mM iodoacetamide, 2 mM phenylmethylsulfonyl fluoride; lysed in lysis buffer containing 100 mM iodoacetamide; and immunoprecipitated. One half of each sample was boiled in SDS-sample buffer with β-mercaptoethanol and the other half without β-mercaptoethanol before gel electrophoresis and autoradiography. The amount of protein present as disulfide-linked aggregates (signal of high molecular weight oligomers as a percentage of total signal for each construct) was quantified by phosphorimager. For analysis in the second-dimension, a lane containing a non-reduced sample was cut out and soaked for 1 minute in sample buffer containing 200 mM β-mercaptoethanol. The gel strip was then loaded horizontally onto a second Tris/tricine SDS-gel, whose stacking gel was supplemented with 50 mM β-mercaptoethanol, and overlaid with reducing sample buffer for electrophoresis.

Immunofluorescence

Transfected cells were grown for 24-72 hours on glass coverslips; fixed with 3% paraformaldehyde for 30 minutes at room temperature; washed in PBS; permeabilized

and blocked with 0.1% saponin, 20 mM glycine and 1% BSA in PBS for 20 minutes; incubated at room temperature with primary antibodies for 2 hours in PBS containing 0.1% saponin, 20 mM glycine and 1% BSA; washed; and stained with fluorescent secondary antibodies in PBS containing 0.1% saponin for 30 minutes After several washes with PBS containing 0.1% saponin, the coverslips were mounted in Mowiol 4-88 (Hoechst). As primary antibodies, we used polyclonal rabbit anti-NPII antiserum, mouse monoclonal anti-myc antibody 9E10, and a mouse monoclonal antibody against the endogenous ER membrane protein BAP31 (a gift from Hans-Peter Hauri; Klumperman et al., 1998). As secondary antibodies, non-cross-reacting Cy3-labeled goat anti-mouse and Cy2-labeled goat anti-rabbit immunoglobulin antibodies (Jackson ImmunoResearch and Amersham Biosciences, respectively) were used according to the manufacturers' recommendations. Staining patterns were analyzed using a Zeiss Axioplan 2 microscope with a Leica DFC420C imaging system or, for Neuro2a cells, with a Zeiss Confocal LSM510 Meta microscope.

Electron microscopy

Cultured cells were fixed in 3% formaldehyde and 0.2% glutaraldehyde for 2 hours at room temperature. After addition of 1% picric acid overnight at 4°C, cells were scraped, pelleted, resuspended and washed three times in PBS, treated with 50 mM NH_4Cl in PBS for 30 minutes to quench free aldehydes, and then washed three times in PBS. The final pellet was resuspended in 2% warm agarose and left on ice to solidify. Agarose pieces were dehydrated and infiltrated with LR-gold resin (London Resin, London, UK) according to the manufacturer's instructions and allowed to polymerize for 1 day at 4°C. For immunogold labeling, sections of about 60 nm were collected on carbon-coated Formvar-Ni-grids, incubated with rabbit anti-NPII in PBS containing 2% BSA and 0.1% Tween-20 for 2 hours, washed with PBS, and incubated with 15-nm colloidal gold-conjugated goat anti-rabbit immunoglobulin antibodies (BioCell, Cardiff) in PBS containing 2% BSA and 0.1% Tween-20 for 90 minutes Grids were washed five times for 5 minutes in PBS and then five times in water before staining for 10 minutes in 2% uranylacetate followed by 1 minute in Reynolds lead citrate solution. Sections were viewed in a Phillips CM100 electron microscope.

For double labeling, the first labeling was performed using rabbit anti-human calreticulin antibody (Stressgen) and 10-nm colloidal gold-conjugated goat anti-rabbit immunoglobulin antibodies as described above. After washing six times for 2 minutes with PBS, the sections were fixed again for 2 hours with 1% formaldehyde and 1% glutaraldehyde in PBS, washed with PBS, and quenched for 10 minutes with 50 mM NH_4Cl. The sections were incubated with PBS containing 2% BSA and 0.1% Tween-20 for 10 minutes, followed by incubation for 90 minutes with rabbit anti-NPII immunoglobulins that had been purified from serum by a protein-A–Sepharose column (Amersham Pharmacia Biotech), pre-coupled to 15-nm gold–protein-A (BioCell) at a molar ratio of 2:1, and incubated with a twofold excess of unrelated mouse IgG. Grids were washed and stained as above. As negative controls to ensure specificity of labeling, cells were stained as above, except that 15-nm gold–protein-A was used that had not been loaded with anti-NPII immunoglobulins. This produced very low background labeling (not shown).

Bacterial expression and in vitro fibril formation

For bacterial expression, the coding sequence of ΔE47 and cysteine-free (abcd) pro-vasopressin (without the signal sequence) were cloned into the plasmid pET21b (Novagen) and thus provided with a C-terminal His6 tag. The proteins were expressed in *E. coli* BL21(DE3) after induction with 1 mM isopropyl-D-thiogalactoside for 2-3 hours, solubilized from inclusion bodies (E47) or the cytosol fraction (abcd) in 8 M urea, 10 mM Tris-HCl pH 8, 1 mM DTT, and protease inhibitors (10 μg/ml each of leupeptin, pepstatin and aprotinin, 0.5 mM orthovanadate, 1 mM PMSF), and purified by Ni-NTA chromatography. Protein at 1 mg/ml was dialyzed stepwise for 8-16 hours each to 6, 5, 4, 2, 1 and 0.5 M urea, and finally to 10 mM Tris-HCl pH 7.4, 100 mM NaCl without DTT overnight. Large precipitates were removed by centrifugation in a tabletop centrifuge for 5 minutes. The supernatant was analyzed by electron microscopy. An aliquot of 10 μl was adsorbed to Formvar carbon-coated Ni grids, washed, dried, stained with 0.5% uranyl acetate for 1 minute, dried, and imaged using a Phillips CM100 electron microscope.

We thank Jane Christensen, Hans-Peter Hauri and Beat Nyfeler for reagents, Christian Appenzeller-Herzog for valuable discussions, and Nicole Beuret for expert technical assistance and advice. This work was supported by grants 3100A0-113319 (to J.R.) and 3100A0-109424 (to M.S.) from the Swiss National Science Foundation, and grant 05A14 (to J.R.) from the Novartis Biomedical Research Foundation.

References

Appenzeller-Herzog, C., Nyfeler, B., Burkhard, P., Santamaria, I., Lopez-Otin, C. and Hauri, H. P. (2005). Carbohydrate- and conformation-dependent cargo capture for ER-exit. *Mol. Biol. Cell* **16**, 1258-1267.

Bergeron, C., Kovacs, K., Ezrin, C. and Mizzen, C. (1991). Hereditary diabetes insipidus: an immunohistochemical study of the hypothalamus and pituitary gland. *Acta. Neuropathol.* **81**, 345-348.

Beuret, N., Rutishauser, J., Bider, M. D. and Spiess, M. (1999). Mechanism of endoplasmic reticulum retention of mutant vasopressin precursor caused by a signal peptide truncation associated with diabetes insipidus. *J. Biol. Chem.* **274**, 18965-18972.

Beuret, N., Stettler, H., Renold, A., Rutishauser, J. and Spiess, M. (2004). Expression of regulated secretory proteins is sufficient to generate granule-like structures in constitutively secreting cells. *J. Biol. Chem.* **279**, 20242-2029.

Braverman, L., Mancini, J. and McGoldrick, D. (1965). Hereditary idiopathic diabetes insipidus in a case report with autopsy findings. *Ann. Intern. Med.* **63**, 503-508.

Castino, R., Davies, J., Beaucourt, S., Isidoro, C. and Murphy, D. (2005). Autophagy is a prosurvival mechanism in cells expressing an autosomal dominant familial neurohypophyseal diabetes insipidus mutant vasopressin transgene. *FASEB J.* **19**, 1021-1023.

Cescato, R., Dumermuth, E., Spiess, M. and Paganetti, P. A. (2000). Increased generation of alternatively cleaved beta-amyloid peptides in cells expressing mutants of the amyloid precursor protein defective in endocytosis. *J. Neurochem.* **74**, 1131-1139.

Chen, L. Q., Rose, J. P., Breslow, E., Yang, D., Chang, W. R., Furey, W. F., Jr, Sax, M. and Wang, B. C. (1991). Crystal structure of a bovine neurophysin II dipeptide complex at 2.8 A determined from the single-wavelength anomalous scattering signal of an incorporated iodine atom. *Proc. Natl. Acad. Sci. USA* **88**, 4240-4244.

Christensen, J. H. and Rittig, S. (2006). Familial neurohypophyseal diabetes insipidus–an update. *Semin. Nephrol.* **26**, 209-223.

Christensen, J. H., Siggaard, C., Corydon, T. J., Robertson, G. L., Gregersen, N., Bolund, L. and Rittig, S. (2004). Impaired trafficking of mutated AVP prohormone in cells expressing rare disease genes causing autosomal dominant familial neurohypophyseal diabetes insipidus. *Clin. Endocrinol.* **60**, 125-136.

Chun, W., Lesort, M., Lee, M. and Johnson, G. V. (2002). Mutant huntingtin aggregates do not sensitize cells to apoptotic stressors. *FEBS Lett.* **515**, 61-65.

Davies, J. and Murphy, D. (2002). Autophagy in hypothalamic neurones of rats expressing a familial neurohypophysial diabetes insipidus transgene. *J. Neuroendocrinol.* **14**, 629-637.

Friberg, M. A., Spiess, M. and Rutishauser, J. (2004). Degradation of wild-type vasopressin precursor and pathogenic mutants by the proteasome. *J. Biol. Chem.* **279**, 19441-19447.

Green, J., Buchan, G., Alvord, E. and Swanson, A. (1967). Hereditary and idiopathic types of diabetes insipidus. *Brain* **90**, 707-714.

Ito, M. and Jameson, J. L. (1997). Molecular basis of autosomal dominant neurohypophyseal diabetes insipidus. Cellular toxicity caused by the accumulation of mutant vasopressin precursors within the endoplasmic reticulum. *J. Clin. Invest.* **99**, 1897-1905.

Ito, M., Oiso, Y., Murase, T., Kondo, K., Saito, H., Chinzei, T., Racchi, M. and Lively, M. O. (1993). Possible involvement of inefficient cleavage of preprovasopressin by signal peptidase as a cause for familial central diabetes insipidus. *J. Clin. Invest.* **91**, 2565-2571.

Klumperman, J., Schweizer, A., Clausen, H., Tang, B. L., Hong, W., Oorschot, V. and Hauri, H. P. (1998). The recycling pathway of protein ERGIC-53 and dynamics of the ER-Golgi intermediate compartment. *J. Cell. Sci.* **111**, 3411-3425.

Lansbury, P. T. and Lashuel, H. A. (2006). A century-old debate on protein aggregation and neurodegeneration enters the clinic. *Nature* **443**, 774-779.

Martinez-Vicente, M. and Cuervo, A. M. (2007). Autophagy and neurodegeneration: when the cleaning crew goes on strike. *Lancet Neurol.* **6**, 352-361.

Nagai, I., Li, C. H., Hsieh, S. M., Kizaki, T. and Urano, Y. (1984). Two cases of hereditary diabetes insipidus, with an autopsy finding in one. *Acta. Endocrinol.* **105**, 318-323.

Nijenhuis, M., Zalm, R. and Burbach, J. P. H. (1999). Mutations in the vasopressin prohormone involved in diabetes insipidus impair endoplasmic reticulum export but not sorting. *J. Biol. Chem.* **274**, 21200-21208.

Olias, G., Richter, D. and Schmale, H. (1996). Heterologous expression of human vasopressin-neurophysin precursors in a pituitary cell line: defective transport of a mutant protein from patients with familial diabetes insipidus. *DNA Cell. Biol.* **15**, 929-935.

Ross, C. A. and Poirier, M. A. (2005). Opinion: What is the role of protein aggregation in neurodegeneration? *Nat. Rev. Mol. Cell. Biol.* **6**, 891-898.

Russell, T. A., Ito, M., Yu, R. N., Martinson, F. A., Weiss, J. and Jameson, J. L. (2003). A murine model of autosomal dominant neurohypophyseal diabetes insipidus reveals progressive loss of vasopressin-producing neurons. *J. Clin. Invest.* **112**, 1697-1706.

Schmale, H. and Richter, D. (1984). Single base deletion in the vasopressin gene is the cause of diabetes insipidus in Brattleboro rats. *Nature* **308**, 705-709.

Si-Hoe, S. L., De Bree, F. M., Nijenhuis, M., Davies, J. E., Howell, L. M., Tinley, H., Waller, S. J., Zeng, Q., Zalm, R., Sonnemans, M. et al. (2000). Endoplasmic reticulum derangement in hypothalamic neurons of rats expressing a familial neurohypophyseal diabetes insipidus mutant vasopressin transgene. *FASEB. J.* **14**, 1680-1684.

Siggaard, C., Rittig, S., Corydon, T. J., Andreasen, P. H., Jensen, T. G., Andresen, B. S., Robertson, G. L., Gregersen, N., Bolund, L. and Pedersen, E. B. (1999). Clinical and molecular evidence of abnormal processing and trafficking of the vasopressin preprohormone in a large kindred with familial neurohypophyseal diabetes insipidus due to a signal peptide mutation. *J. Clin. Endocrinol. Metab.* **84**, 2933-2941.

Willcutts, M. D., Felner, E. and White, P. C. (1999). Autosomal recessive familial neurohypophyseal diabetes insipidus with continued secretion of mutant weakly active vasopressin. *Hum. Mol. Genet.* **8**, 1303-1307.